Feature of Exact Exchange Kohn–Sham Orbitals with Krieger–Li–Iafrate Approximation#

Jaewook Kim, Kwangwoo Hong, Sunghwan Choi, and Woo Youn Kim*

*Department of Chemistry, KAIST, Daejeon 305-701, Korea. *E-mail: wooyoun@kaist.ac.kr*
Received November 11, 2014, Accepted December 20, 2014, Published online February 20, 2015

We report feature of Kohn–Sham (KS) molecular orbitals computed with the Krieger–Li–Iafrate (KLI) approximation for exact exchange through the comparison to the results of Hartree–Fock (HF) and other KS methods such as local density approximation (LDA) and generalized gradient approximation (GGA). KLI occupied orbitals have similar energies and shapes with those of HF. KLI virtual orbitals are likely to form bound states with negative eigenvalues due to the correct $-1/r$ asymptotic behavior of KLI potentials, whereas HF virtual orbitals are mostly unbound. As a result, HF orbitals tend to be diffuse because of their plane-wave-like nature, and their energies are highly sensitive to the size of basis set. The energies of LDA/GGA orbitals appear to be upshifted by a constant factor from the KLI results, but they also produce unbound virtual orbitals like HF. The energy gaps between KLI occupied and virtual orbitals are very close to the corresponding experimental excitation energies compared to the other methods. We also show that Brillouin's theorem can be applied to a Slater determinant made of KLI orbitals as a corollary of the KLI approximation.

Keywords: Density functional theory, Exact exchange, Optimized effective potential, Krieger–Li–Iafrate approximation, Kohn–Sham orbitals, Brillouin's theorem, Configuration interactions

Introduction

Kohn–Sham density functional theory (KS-DFT) provides an efficient single determinant method with reliable accuracy for electronic structure calculations of atoms, molecules, and solids. The tremendous success of KS-DFT in computational physics and chemistry is apparently thanks to the active development of accurate functionals using the local density approximation (LDA) and generalized gradient approximation (GGA).[1–3] However, such conventional functionals suffer from the notorious self-interaction error (SIE), which causes serious problems in DFT computations: *e.g.*, diffuse KS orbitals, high orbital energies, small bandgap energies, and even wrong ground states for strongly correlated systems.[3–5] In addition, conventional exchange-correlation potentials decay exponentially and thus fail to reproduce the correct $-1/r$ asymptotic behavior, which is essential to correctly describe Rydberg states, electron affinities, and charge-transfer excitations.[3,5,6] Because those problems are due to the absence of exact exchange (EXX), hybrid functionals created by mixing the Hartree–Fock (HF) exchange and GGAs according to the adiabatic connection theory partly alleviated them and soon became a method of choice especially in chemistry.[1–4]

Unlike the nonlocal HF exchange, the KS potential should be local and equal for all the electrons in a given system. The optimized effective potential (OEP) method enables us to generate a local potential from the HF exchange, resulting in an EXX KS potential.[7–11] In practice, various approximated methods such as the Krieger–Li–Iafrate (KLI),[12–15] localized HF,[16–18] and common energy denominator approximations[19,20] have been developed to avoid the numerical difficulty in solving the OEP integral equation. More recently, the orbital-consistent and density-consistent effective potentials have been proposed as a practical alternative.[21,22] However, use of OEP methods in real applications has been limited, because there have been no appropriate counterparts for correlation energies: the errors including the SIE in conventional correlation functionals cannot be canceled out by EXX methods. Ultimately, therefore, exchange-only OEP methods should be combined with correct correlation methods.

In this regard, it appears a natural extension to develop accurate correlation methods in the basis of EXX DFT. On one hand, according to the hierarchy of the Jacob's ladder for DFT accuracy,[23,24] the random phase approximation has been used widely to calculate correlation energies as a counterpart of EXX methods.[25–31] Recently, a correlation version of the OEP method has been developed.[32–37] On the other hand, multiconfiguration (MC) methods can be exploited to take especially the nondynamical correlation energies into account. The following two approaches were proposed. The first one uses kinetic and electron–electron interaction energies from post-HF calculations and generates the electron density directly from a corresponding many-electron wavefunction.[38–49] Then, residual dynamical correlation energies are corrected by using the conventional correlation functionals in DFT. However, the double counting of correlation energies is inevitable in this approach. Range-separation treatment of Coulomb interactions[39,43,46,47] or pair-density functionals[38,40,44,46,47] may be used to resolve it. The second

This paper is dedicated to Professor Kwan Kim on the occasion of his honorable retirement.

approach replaces HF orbitals by KS orbitals as a basis for MC expansions. (Multireference) Configuration interaction calculations from KS orbitals showed faster convergence in terms of the size of reference spaces than those from HF orbitals.[50–56] Gutlé *et al*. reported that a coupled-cluster (CC) method using KS orbitals obtained from the KLI approximation has shown rapid energy convergence for atomic systems with similar accuracy compared to the HF-based CC method.[57,58] These previous studies may indicate promising applicability of KS orbitals to MC methods. Unfortunately, however, Slater determinants derived from KS orbitals do not hold Brillouin's theorem, which is relevant to the computational efficiency in the evaluation of two-electron integrals between Slater determinants.

In the present work, we investigate whether KS orbitals computed from the KLI approximation can be a good reference configuration for correlation energy calculations using MC methods. To be self-contained and clarify the feature of the KLI approximation, we revisit the OEP derivation using perturbation theory and explain the numerical implementation of the KLI method into our DFT code that uses Lagrange-sinc functions as a basis set.[59] Subsequently, we compare the shape and energy of the occupied and virtual orbitals obtained from the HF, LDA, GGA, and KLI methods with each other. We also compare the KS total energy and the ground state energy from the configuration interaction singles (CIS) using KS orbitals to examine the validity of Brillouin's theorem. Finally, we address a future outlook of the KLI method toward MC approaches.

Theory

Derivation of the OEP and KLI Methods. In general, the exact exchange-correlation energy (E_{xc}) in DFT may be a nonlocal functional of the electron density, though many conventional LDA, GGA, and meta-GGA functionals are either local or semilocal. Hybrid functionals partly include those features with the parameters optimized. The OEP method offers a rigorous way to obtain a local KS potential (V_{KS}) from a nonlocal exchange-correlation energy.[9–11] Because the exact expression of the exchange energy is known, as shown in Eq. (1), one can readily obtain an exchange-only potential (V_x) using the OEP method.

$$E_x^{HF}[\{\varphi_{i\sigma}\}] = -\frac{1}{2}\sum_{\sigma}\sum_{i,j=1}^{N_\sigma}\int\int d\mathbf{r}d\mathbf{r}'\frac{\varphi_{i\sigma}^*(\mathbf{r})\varphi_{j\sigma}^*(\mathbf{r}')\varphi_{j\sigma}(\mathbf{r})\varphi_{i\sigma}(\mathbf{r}')}{|\mathbf{r}-\mathbf{r}'|}, \quad (1)$$

where $\{\varphi_{i\sigma}\}$ is a set of KS or HF orbitals, and N_σ is the number of electrons with spin σ. Here, we derive the OEP method for the exchange-only case using perturbation theory and subsequently obtain a formal expression of V_x under the KLI approximation.

KS-DFT, in principle, gives the exact ground state energy and density of a noninteracting system that is identical to those of a corresponding interacting system.[60] Assuming an interacting system with only the Hartree and exchange interactions between electrons, a corresponding KS reference system should have the ground state energy and density identical to HF results:

$$n_\sigma^{HF}(\mathbf{r}) = n_\sigma^{KS}(\mathbf{r}), \quad E^{HF}[\{\varphi_{i\sigma}\}] = E^{KS}\left[n_\sigma^{KS}\right], \quad (2)$$

where both HF and KS spin densities $n_\sigma(\mathbf{r})$ can be represented with HF and KS orbitals $\{\varphi_{i\sigma}\}$, respectively, as follows:

$$\hat{F}_\sigma^{HF}\left[\{\varphi_{i\sigma}^{HF}\}\right]\varphi_{i\sigma}^{HF} = \epsilon_{i\sigma}^{HF}\varphi_{i\sigma}^{HF}, \quad n_\sigma^{HF}(\mathbf{r}) = \sum_i^{N_\sigma}\left|\varphi_{i\sigma}^{HF}(\mathbf{r})\right|^2 \quad (3)$$

and

$$\hat{H}_\sigma^{KS}\varphi_{i\sigma}^{KS} = \epsilon_{i\sigma}^{KS}\varphi_{i\sigma}^{KS}, \quad n_\sigma^{KS}(\mathbf{r}) = \sum_i^{N_\sigma}\left|\varphi_{i\sigma}^{KS}(\mathbf{r})\right|^2, \quad (4)$$

where $\epsilon_{i\sigma}$ is the energy of the corresponding orbital $\varphi_{i\sigma}$. Note that the Fock operator F^{HF} is used in Eq. (3), while the exchange-only KS Hamiltonian H^{KS} is used in Eq. (4). If both HF and KS densities are identical, the difference between $\hat{F}_\sigma^{HF}$ and $\hat{H}_\sigma^{KS}$ solely comes from their exchange parts:

$$\hat{F}_\sigma^{HF}\left[\{\varphi_{i\sigma}^{HF}\}\right] - \hat{H}_\sigma^{KS} \equiv \hat{v}_x^{HF} - \hat{v}_x^{OEP}, \quad (5)$$

where $\hat{v}_x^{HF}$ and $\hat{v}_x^{OEP}$ denote the HF exchange operator (Eq. (6)) and the exchange-only OEP, respectively.

$$\begin{aligned} v_{x,i\sigma}^{HF}[\{\varphi_{i\sigma}\}](\mathbf{r}) &= \frac{1}{\varphi_{i\sigma}^*(\mathbf{r})}\frac{\delta E_x^{HF}[\{\varphi_{i\sigma}\}]}{\delta\varphi_{i\sigma}(\mathbf{r})} \\ &= -\frac{1}{\varphi_{i\sigma}^*(\mathbf{r})}\sum_{j=1}^{N_\sigma}\varphi_{j\sigma}^*(\mathbf{r})\int d\mathbf{r}'\frac{\varphi_{i\sigma}^*(\mathbf{r}')\varphi_{j\sigma}(\mathbf{r}')}{|\mathbf{r}-\mathbf{r}'|} \end{aligned} \quad (6)$$

As indicated in Eq. (6), the Hartree exchange potential is spin–orbital-dependent and thus should be labeled with $i\sigma$ (*i.e.*, $v_{x,i\sigma}^{HF}$). Using Eq. (6), the HF exchange energy in Eq. (1) can be written as

$$E_x^{HF}[\{\varphi_{i\sigma}\}] = \sum_\sigma\sum_{i=1}^{N_\sigma}\left\langle\varphi_{i\sigma}\middle|\hat{v}_{x,i\sigma}^{HF}[\{\varphi_{i\sigma}\}]\middle|\varphi_{i\sigma}\right\rangle. \quad (7)$$

For an arbitrary KS Hamiltonian, its ground state energy and density may be different from the corresponding HF results. Then, we add a small perturbation Δv on the given KS potential so as to minimize their energy and density difference. By taking perturbative corrections up to the first order, the modified KS equation reads

$$\begin{aligned} &\left(\hat{H}_\sigma^{KS} + \lambda\Delta v\right)\left(\varphi_{i\sigma}^{KS} + \lambda\varphi_{i\sigma}^{(1)} + \mathcal{O}(\lambda^2)\right) \\ &= \left(\epsilon_{i\sigma}^{KS} + \lambda\epsilon_{i\sigma}^{(1)} + \mathcal{O}(\lambda^2)\right)\left(\varphi_{i\sigma}^{KS} + \lambda\varphi_{i\sigma}^{(1)} + \mathcal{O}(\lambda^2)\right) \end{aligned} \quad (8)$$

and the resulting spin density becomes

$$\begin{aligned} n_\sigma^{\mathrm{KS}}(\mathbf{r}) &= \sum_i^{N_\sigma} \left| \varphi_{i\sigma}^{\mathrm{KS}}(\mathbf{r}) + \lambda \varphi_{i\sigma}^{(1)}(\mathbf{r}) + \mathcal{O}(\lambda^2) \right|^2 \\ &= \sum_i^{N_\sigma} \left\{ \left| \varphi_{i\sigma}^{\mathrm{KS}}(\mathbf{r}) \right|^2 + \left(\lambda \varphi_{i\sigma}^{(1)*}(\mathbf{r}) \varphi_{i\sigma}^{\mathrm{KS}}(\mathbf{r}) + \text{c.c.} \right) \right\} + \mathcal{O}(\lambda^2), \end{aligned} \tag{9}$$

where λ indicates a bookkeeping order parameter, $\varphi_{i\sigma}^{(1)}$ denotes the first-order correction to a KS orbital $\varphi_{i\sigma}^{\mathrm{KS}}$ that is given as

$$\varphi_{i\sigma}^{(1)}(\mathbf{r}) = \sum_{k=1, k\neq i}^{\infty} \frac{\langle \varphi_{k\sigma}^{\mathrm{KS}} | \Delta v | \varphi_{i\sigma}^{\mathrm{KS}} \rangle}{\varepsilon_{k\sigma}^{\mathrm{KS}} - \varepsilon_{i\sigma}^{\mathrm{KS}}} \varphi_{k\sigma}^{\mathrm{KS}}(\mathbf{r}), \tag{10}$$

and $\epsilon_{i\sigma}^{(1)}$ is the first-order correction to the corresponding KS orbital energy, which is given as

$$\begin{aligned} \epsilon_{i\sigma}^{(1)} &= \langle \varphi_{i\sigma}^{\mathrm{KS}} | \Delta \mathrm{v} | \varphi_{i\sigma}^{\mathrm{KS}} \rangle = \left\langle \varphi_{i\sigma}^{KS} \middle| \hat{\mathrm{v}}_{\mathrm{x},i\sigma}^{\mathrm{HF}} - \hat{\mathrm{v}}_{\mathrm{x}}^{\mathrm{OEP}} \middle| \varphi_{i\sigma}^{\mathrm{KS}} \right\rangle \\ &\equiv \bar{\mathrm{v}}_{\mathrm{x},i\sigma}^{\mathrm{HF}} - \bar{\mathrm{v}}_{\mathrm{x},i\sigma}^{\mathrm{OEP}}. \end{aligned} \tag{11}$$

Here we used the fact that the perturbative potential Δv is just the potential difference in Eq. (5). Replacing the spin density in Eq. (2) by Eq. (9), the so-called OEP integral equation can be obtained as

$$\begin{aligned} 0 &= n_\sigma^{\mathrm{KS}}(\mathbf{r}) - n_\sigma^{\mathrm{HF}}(\mathbf{r}) \\ &= \sum_i^{N_\sigma} \left\{ \left| \varphi_{i\sigma}^{\mathrm{KS}}(\mathbf{r}) \right|^2 + \left(\lambda \varphi_{i\sigma}^{(1)*}(\mathbf{r}) \varphi_{i\sigma}^{\mathrm{KS}}(\mathbf{r}) + \text{c.c.} \right) \right\} \\ &\quad - \sum_i^{N_\sigma} \left| \varphi_{i\sigma}^{\mathrm{HF}}(\mathbf{r}) \right|^2 + \mathcal{O}(\lambda^2) \\ &= \lambda \sum_i^{N_\sigma} \left(\varphi_{i\sigma}^{(1)*}(\mathbf{r}) \varphi_{i\sigma}^{\mathrm{KS}}(\mathbf{r}) + \text{c.c.} \right) + \mathcal{O}(\lambda^2) \end{aligned} \tag{12}$$

To obtain an explicit expression of $v_{\mathrm{x}}^{\mathrm{OEP}}$, Eq. (8) can be rewritten as

$$\begin{aligned} &\hat{H}_\sigma^{\mathrm{KS}} \varphi_{i\sigma}^{\mathrm{KS}} + \lambda \Delta v \varphi_{i\sigma}^{\mathrm{KS}} + \hat{H}_\sigma^{\mathrm{KS}} \lambda \varphi_{i\sigma}^{(1)} = \\ &\epsilon_{i\sigma}^{\mathrm{KS}} \varphi_{i\sigma}^{\mathrm{KS}} + \lambda \epsilon_{i\sigma}^{\mathrm{KS}} \varphi_{i\sigma}^{(1)} + \lambda \epsilon_{i\sigma}^{(1)} \varphi_{i\sigma}^{\mathrm{KS}} + \mathcal{O}(\lambda^2). \end{aligned} \tag{13}$$

The first terms on both sides in Eq. (13) cancel out because of Eq. (4). Therefore, by ignoring the higher order terms, Eq. (13) can be rearranged as

$$\begin{aligned} \left(\Delta \mathrm{v} - \epsilon_{\mathrm{i}\sigma}^{(1)} \right) \varphi_{\mathrm{i}\sigma}^{\mathrm{KS}} &= \left(\epsilon_{\mathrm{i}\sigma}^{\mathrm{KS}} - \hat{\mathrm{H}}_\sigma^{\mathrm{KS}} \right) \varphi_{\mathrm{i}\sigma}^{(1)} \\ &= \left(\epsilon_{\mathrm{i}\sigma}^{\mathrm{KS}} + \frac{1}{2}\nabla^2 - \hat{\mathrm{v}}_\sigma^{\mathrm{KS}} \right) \varphi_{\mathrm{i}\sigma}^{(1)}. \end{aligned} \tag{14}$$

After multiplying $\hat{\mathrm{v}}_\sigma^{\mathrm{KS}}$ to the last line in Eq. (12) and substituting Eq. (14) into the result, we arrive at

$$\begin{aligned} 0 &= \hat{v}_\sigma^{\mathrm{KS}} \sum_i^{N_\sigma} \varphi_{i\sigma}^{(1)^*}(\mathbf{r}) \varphi_{i\sigma}^{\mathrm{KS}}(\mathbf{r}) + \text{c.c.} \\ &= \sum_i^{N_\sigma} \left\{ \left(\varepsilon_{i\sigma}^{\mathrm{KS}} + \frac{1}{2}\nabla^2 \right) \varphi_{i\sigma}^{(1)^*}(\mathbf{r}) \varphi_{i\sigma}^{\mathrm{KS}}(\mathbf{r}) \right. \\ &\quad \left. - \left(\Delta v(\mathbf{r}) - \epsilon_i^{(1)} \right) \varphi_{i\sigma}^{\mathrm{KS}\,*}(\mathbf{r}) \varphi_{i\sigma}^{\mathrm{KS}}(\mathbf{r}) \right\} + \text{c.c.}. \end{aligned} \tag{15}$$

Rearranging the above equation to obtain $v_{\mathrm{x}}^{\mathrm{OEP}}$, we have

$$\begin{aligned} v_{\mathrm{x},\sigma}^{\mathrm{OEP}}(\mathbf{r}) = \frac{1}{2\rho_\sigma(\mathbf{r})} \sum_i^{N_\sigma} \left\{ \left(\varepsilon_{i\sigma} + \frac{1}{2}\nabla^2 \right) \varphi_{i\sigma}^{(1)*}(\mathbf{r}) \varphi_{i\sigma}^{\mathrm{KS}}(\mathbf{r}) \right. \\ \left. + \left| \varphi_{i\sigma}^{\mathrm{KS}}(\mathbf{r}) \right|^2 \left(v_{\mathrm{x},i\sigma}^{\mathrm{HF}}(\mathbf{r}) - \left(\bar{v}_{\mathrm{x},i\sigma}^{\mathrm{HF}} - \bar{v}_{x,i\sigma}^{\mathrm{OEP}} \right) \right) \right\} + \text{c.c.} \end{aligned} \tag{16}$$

which can be solved iteratively.[10,61] The most time-consuming part in solving Eq. (16) is the evaluation of the first-order orbital correction $\varphi_{i\sigma}^{(1)^*}(\mathbf{r})$, because it demands the summation over the whole orbital space [cf. Eq. (10)]. The KLI approximation assumes that

$$\langle \varphi_{k\sigma}^{\mathrm{KS}} | \Delta v | \varphi_{i\sigma}^{\mathrm{KS}} \rangle = 0 \quad \text{for all } k \neq i. \tag{17}$$

Then the Eq. (16) becomes much simpler because $\varphi_{i\sigma}^{(1)*}(\mathbf{r})$ becomes zero:

$$\begin{aligned} &v_{\mathrm{x},\sigma}^{\mathrm{OEP}}(\mathbf{r}) \\ &\approx \frac{1}{\rho_\sigma(\mathbf{r})} \sum_i^{N_\sigma} \left| \varphi_{i\sigma}^{\mathrm{KS}}(\mathbf{r}) \right|^2 \left(v_{\mathrm{x},i\sigma}^{\mathrm{HF}}(\mathbf{r}) - \left(\bar{v}_{\mathrm{x},i\sigma}^{\mathrm{HF}} - \bar{v}_{\mathrm{x},i\sigma}^{\mathrm{OEP}} \right) \right). \end{aligned} \tag{18}$$

Finally, we define the KLI exchange-only potential $v_{\mathrm{x}}^{\mathrm{KLI}}$ as follows:

$$v_{x,\sigma}^{\mathrm{KLI}}(\mathbf{r}) \equiv \frac{1}{\rho_\sigma(\mathbf{r})} \sum_i^{N_\sigma} \left| \varphi_{i\sigma}^{\mathrm{KS}}(\mathbf{r}) \right|^2 \left(v_{x,i\sigma}^{\mathrm{HF}}(\mathbf{r}) - \left(\bar{v}_{x,i\sigma}^{\mathrm{HF}} - \bar{v}_{x,i\sigma}^{\mathrm{KLI}} \right) \right). \tag{19}$$

Note that the KLI exchange potential depends only on the occupied orbitals. One may wonder that ignoring the entire term in Eq. (10) appears a very crude approximation, but many previous studies with the KLI approximation have shown astonishingly accurate results.[21,22,62–64] In fact, the KLI approximation can be considered as a mean-field approximation assuming a slowly varying density.[65]

Unlike Eq. (12), Eq. (19) can be readily solved.[13–15] To this end, we need to evaluate the orbital-averaged KLI potential $\bar{v}_{\mathrm{x},i\sigma}^{\mathrm{KLI}} = \left\langle \varphi_{i\sigma} \middle| v_{\mathrm{x},\sigma}^{\mathrm{KLI}} \middle| \varphi_{i\sigma} \right\rangle$. From Eq. (19)

$$\bar{v}_{\mathrm{x},i\sigma}^{\mathrm{KLI}} = \bar{v}_{\mathrm{x},i\sigma}^{\mathrm{S}} - \sum_j^{N_\sigma - 1} M_{ji\sigma} \left(\bar{v}_{\mathrm{x},j\sigma}^{\mathrm{HF}} - \bar{v}_{\mathrm{x},j\sigma}^{\mathrm{KLI}} \right), \tag{20}$$

where $\bar{v}^{S}_{x,i\sigma} = \left\langle \varphi_{i\sigma} \middle| v^{S}_{x,\sigma} \middle| \varphi_{i\sigma} \right\rangle$ is the orbital-averaged value of the Slater potential[66]

$$v^{S}_{x,\sigma} \equiv \sum_{i}^{N_\sigma} \frac{|\varphi_{i\sigma}(\mathbf{r})|^2}{\rho_\sigma(\mathbf{r})} v^{HF}_{x,i\sigma}(\mathbf{r}) \tag{21}$$

and

$$M_{ji\sigma} \equiv \int d\mathbf{r} \frac{|\varphi_{j\sigma}(\mathbf{r})|^2 |\varphi_{i\sigma}(\mathbf{r})|^2}{\rho_\sigma(\mathbf{r})}. \tag{22}$$

The summation in Eq. (20) omits the term for $j = N_\sigma$ because of the asymptotic behavior of electron density as $\mathbf{r} \to \infty$. Since $\rho_\sigma(\mathbf{r}) \sim |\varphi_{N_\sigma\sigma}(\mathbf{r})|^2$ as $\mathbf{r} \to \infty$, $v^{KLI}_{x,\sigma}(\mathbf{r})$ can be written as

$$v^{KLI}_{x,\sigma}(\mathbf{r}) \sim v^{HF}_{x,N_\sigma\sigma}(\mathbf{r}) - \left(\bar{v}^{HF}_{x,N_\sigma\sigma} - \bar{v}^{KLI}_{x,N_\sigma\sigma} \right). \tag{23}$$

$v^{HF}_{x,N_\sigma\sigma}(\mathbf{r})$ goes to zero as $\mathbf{r} \to \infty$ and thus we can choose that $v^{KLI}_{x,\sigma}(\mathbf{r})$ also goes to zero as $\mathbf{r} \to \infty$. Then, Eq. (23) should satisfy

$$\bar{v}^{HF}_{x,N_\sigma\sigma} - \bar{v}^{KLI}_{x,N_\sigma\sigma} = 0. \tag{24}$$

To evaluate $\bar{v}^{HF}_{x,j\sigma} - \bar{v}^{KLI}_{x,j\sigma}$ for $j < N_\sigma$, Eq. (20) can be rearranged to obtain a linear equation for $\bar{v}^{HF}_{x,j\sigma} - \bar{v}^{KLI}_{x,j\sigma}$:

$$\sum_{j}^{N_\sigma - 1} \left(\delta_{ji} - M_{ji\sigma} \right) \left(\bar{v}^{HF}_{x,j\sigma} - \bar{v}^{KLI}_{x,j\sigma} \right) = \bar{v}^{HF}_{x,i\sigma} - \bar{v}^{S}_{x,i\sigma}. \tag{25}$$

Brillouin's Theorem. For the HF ground state wavefunction, $|\Psi_0\rangle$, the Brillouin's theorem states that

$$\begin{aligned} \left\langle \Psi_0 \middle| \hat{H} \middle| \Psi^a_i \right\rangle &= \left\langle i \middle| \hat{h} \middle| a \right\rangle + \sum_k \langle ik || ak \rangle \\ &= \left\langle i \middle| \hat{F}^{HF} \middle| a \right\rangle = 0, \end{aligned} \tag{26}$$

where $\left| \Psi^a_i \right\rangle$ is the one-particle excitation wavefunction created by replacing the ith occupied orbital of the ground state determinant by the ath virtual orbital. However, for a KS ground state determinant Brillouin's theorem does not hold, because the KS orbitals are not the eigenfunctions of the Fock operator.

As shown in Eq. (5), the difference between $\hat{F}^{HF}$ and the exchange-only $\hat{H}^{KS}$ is in their exchange parts and thus $\left\langle i \middle| \hat{F}^{HF} \middle| a \right\rangle$ in Eq. (26) can be written as

$$\begin{aligned} \left\langle i \middle| \hat{F}^{HF} \middle| a \right\rangle &= \left\langle i \middle| \hat{H}^{KS} \middle| a \right\rangle + \left\langle i \middle| \hat{v}^{HF}_x - \hat{v}^{KS}_{x\sigma} \middle| a \right\rangle \\ &= \left\langle i \middle| \hat{v}^{HF}_x - \hat{v}^{KS}_{x\sigma} \middle| a \right\rangle. \end{aligned} \tag{27}$$

The KLI approximation assumes that the last term in Eq. (27) is zero as in the case of Eq. (17). Therefore, Slater determinants made up of KS orbitals obey Brillouin's theorem within the KLI approximation.

Implementation and Calculation Details

We implemented the KLI exchange potential in Eq. (19) in our DFT code using Lagrange-sinc functions as a basis set.[59] Lagrange functions are a set of localized real-space basis functions that satisfy orthonormality and cardinality.[67–69] Using Lagrange functions as a basis set, only the diagonal matrix elements of a local potential (*e.g.*, v^{KLI}_x) are nonzero due to the cardinality:

$$\left\langle L_i \middle| V^{KLI}_x \middle| L_{i'} \right\rangle = \int L^*_i(x) V^{KLI}_x(x) L_{i'}(x)\, dx = V^{KLI}_x(x_i)\delta_{ii'}, \tag{28}$$

where $L_i(x)$ is a Lagrange function localized on the ith Lagrange mesh point.

The KLI potential is calculated using the Eqs. (6), (19), (21), (22), and (25). To perform the integral for the Coulomb potential ($1/r_{12}$) in Eq. (6), we employed the interpolating scaling function method,[70,71] which replaces the Coulomb potential by the integration of a Gaussian function as

$$\begin{aligned} &\int d\mathbf{r}' \frac{\varphi^*_{\mu\sigma}(\mathbf{r}')\varphi_{\nu\sigma}(\mathbf{r}')}{|\mathbf{r}-\mathbf{r}'|} \\ &= \frac{2}{\sqrt{\pi}} \int_0^\infty dt \int d\mathbf{r}' \varphi^*_{\mu\sigma}(\mathbf{r}')\varphi_{\nu\sigma}(\mathbf{r}') e^{-t^2(\mathbf{r}-\mathbf{r}')^2} \\ &= \frac{2}{\sqrt{\pi}} \sum_a w_a \sum_i F^{x,a}_{i'i} \sum_j F^{y,a}_{j'j} \sum_k F^{z,a}_{k'k} d_{ijk}, \end{aligned} \tag{29}$$

where $F^{x,a}_{i'i}$, $F^{y,a}_{j'j}$, and $F^{z,a}_{k'k}$ are called the Poisson matrix elements, *e.g.*,

$$F^{x,a}_{i'i} = \int_{-\infty}^{\infty} e^{-t_a^2(x_{i'}-x)^2} L_i(x)\, dx$$

and d_{ijk}, w_a, and t_a are the coefficients of Lagrange functions, a weight factor, and a quadrature point of the Gaussian integral, respectively. In the evaluation of Eqs. (6), (21), and (22), vanishing of the electron density or orbitals may cause a numerical problem.[16] Thus, we use $v^{HF}_{x,i\sigma}(\mathbf{r})\varphi^*_{i\sigma}(\mathbf{r})$ instead of $v^{HF}_{x,i\sigma}(\mathbf{r})$. Also, the KLI exchange potential at a remote region where the spin density is $<10^{-10}$ a.u. is approximated as[16]

$$v^{KLI}_{x,\sigma}(\mathbf{r}) \approx \frac{1}{N_\sigma} \int d\mathbf{r}' \frac{\rho_\sigma(\mathbf{r}')}{|\mathbf{r}-\mathbf{r}'|}. \tag{30}$$

In what follows, we compare the orbital energies and shapes of four small molecules (H_2, N_2, CO, and CH_4) obtained from the KLI, HF, PZ-LDA,[72–74] and PBE[75] methods. Their geometries were obtained from Ref. 76. We used the Gaussian

09 package for calculations using the cc-pVDZ and aug-cc-pVQZ basis sets.[77] For KS-DFT calculations, we also used our code with the Lagrange-sinc basis set[59] and norm-conserving pseudopotentials.[78] For details of our code, refer to Ref. 59. For KLI calculations, we adopted the pseudopotentials generated at the PBE level. For the Lagrange-sinc basis set, we used a spherical-shaped simulation box of 10 bohr radius with a scaling factor $h = 0.20$ or 0.25 bohr. To accelerate the SCF convergence, we use a potential mixing scheme in DFT calculations with the KLI potential. We use VESTA with the isovalue of 0.02 to draw molecular orbitals.[79]

Results and Discussion

Comparison of Orbital Energies. To elucidate the feature of KLI orbitals, we first compare the orbital energies of N_2 computed from KLI with those from the other methods. Figure 1 shows the results. First of all, the KLI-occupied orbital energies are close to those of HF. In particular, the highest occupied molecular orbital (HOMO) energy should be equal to that of HF if the same basis set is used for both KLI and HF [see Eq. (24)], though in Figure 1 there is a slight deviation (0.0156 a.u. in the case of HF with aug-cc-pVQZ). In fact, the KLI and HF HOMO energies for other molecules (H_2, CO, and CH_4) show even smaller deviations (0.003–0.004 a.u.). Therefore, as in HF, the KLI HOMO energy can be a good approximated ionization energy. Note that the $3\sigma_g$ orbital should be the HOMO of N_2, but HF assigns $1\pi_u$ as the HOMO. This is a well-known limitation of HF.[80–82]

In contrast, the KLI virtual orbital energies are much lower than those of HF. It has been known that virtual orbital energies of HF correspond to the electron affinity (*i.e.*, Koopmans' theorem), which causes that an electron in a virtual orbital tends to form an unbound state due to the strong repulsion from the N electrons in the occupied orbitals, as depicted in Figure 1. However, KS orbitals do not satisfy Koopmans' theorem and also both occupied and virtual orbitals share the same KS potential that is made from the electron density of the occupied orbitals. Thus, electrons in a virtual orbital see $N-1$ electrons as those in the occupied orbitals. Consequently, the energy gaps between the KS occupied and virtual orbitals are close to the corresponding optical excitation energies. Indeed, the KLI transition energies from HOMO to $1\pi_g$ and to $4\sigma_g$ are very close to corresponding experimental values, respectively, as shown in Figure 1. Note that PBE also produces unbound virtual orbitals like HF. We also compared PZ-LDA results, and they are very close to the PBE results (the maximum difference of orbital energies is 0.0098 a.u.). This is because of the shallow LDA/GGA exchange-correlation potentials due to the SIE (*e.g.*, see Figure 2).[6,83]

Interestingly, the PBE-occupied orbital energies with a constant downshift are similar to the KLI values as already reported.[6,83–86] Their virtual orbital energies still show significant deviation and it gets worse as the orbital energy increases. This can be understood as follows. In the region of valence electrons, LDA/GGA potentials have similar

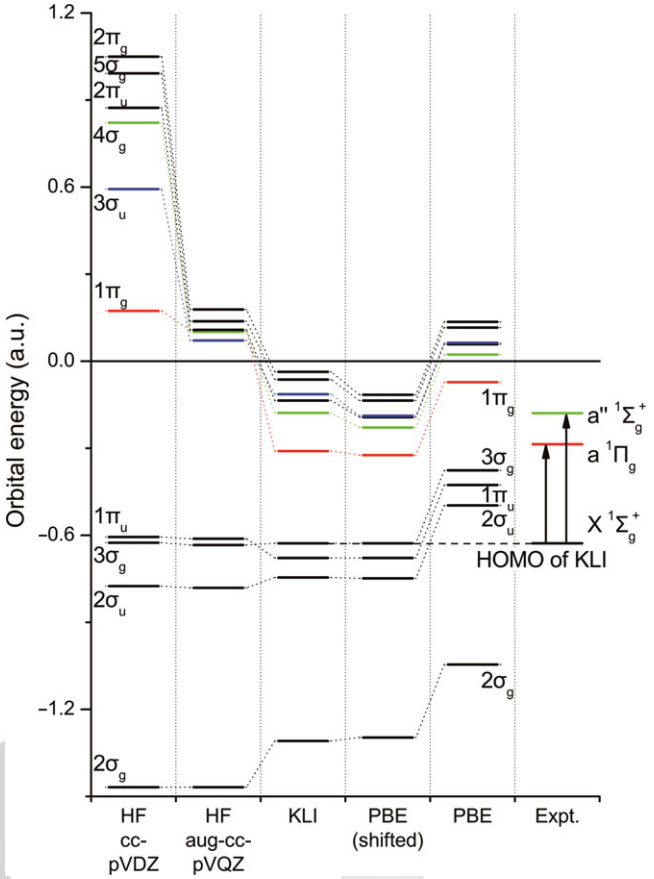

Figure 1. Orbital energies of N_2. The dotted lines connect the orbitals with the same symmetry, while the dashed line denotes the KLI HOMO energy. Because the energy order of HF orbitals is different from that of KS orbitals, we exclude some of HF virtual orbitals. PBE (shifted) indicates the orbital energies with constant downshift. For comparison, selected experimental singlet excitation energies are present with respect to the KLI HOMO energy.[88] All the KS orbital energies have been calculated using the Lagrange- sinc basis set with the scaling factor of 0.25 bohr.

curvature to that of KLI, leading to the relatively small energy difference for the occupied orbitals. In a remote region, the LDA/GGA potentials decay exponentially, while the KLI potential shows $-1/r$ asymptotic tail (*e.g.*, see Figure 2), resulting in large energy differences for virtual orbitals.

Basis Set Dependence of Virtual Orbitals. In Figure 1, HF virtual orbital energies of N_2 are strongly dependent on the size of basis set. Those orbitals form unbound states, as mentioned above, and thus tend to be delocalized as long as the given basis set allows. Table 1 shows such examples. HF orbitals of N_2 computed from aug-cc-pVQZ are much more diffuse than the corresponding orbitals from cc-pVDZ, as the former contains diffuse functions whereas the latter does not. In the case of $4\sigma_g$, even their geometries are qualitatively different. As a result, the orbital energies with cc-pVDZ are much higher than those with aug-cc-pVQZ. Similar tendency is observed in PBE unbound orbitals ($4\sigma_g$ and $3\sigma_u$), but the bound virtual orbital $1\pi_g$ of PBE shows no significant change. In fact, the

shape of unbound orbitals is entirely determined by the basis set size, because they have plane-wave-like nature. If more diffuse functions are added to a given basis set, the resulting orbitals will be more delocalized and accordingly their energies become closer to zero.

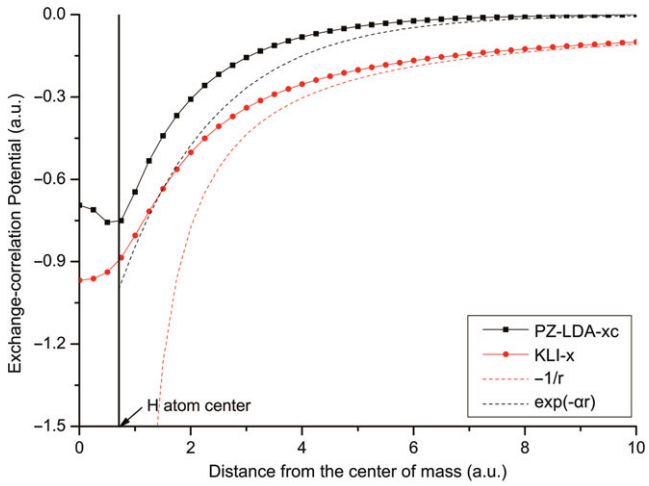

Figure 2. Comparison of the PZ-LDA exchange-correlation potential and the KLI exchange potential for H_2. The dotted lines indicate the asymptotic behavior of the corresponding potentials. The decay constant α of the LDA asymptotic potential was determined from the HOMO energy as $\alpha \approx \sqrt{8\epsilon_{HOMO}/9}$.[3,6,89]

Grid-based basis sets such as the Lagrange-sinc functions can readily describe diffuse functions without additional costs. Table 1 also shows virtual orbitals computed from the Lagrange-sinc basis set. The PBE $1\pi_g$ and $3\sigma_u$ orbitals from the Lagrange-sinc basis set have slightly different shapes compared to those from aug-cc-pVQZ. However, $4\sigma_g$ from the former is more diffuse along the perpendicular direction to the bond axis, while that from the latter is more diffuse along the parallel direction to the bond axis. We suspect that such a difference is due to undesirable constraints of aug-cc-pVQZ, because the Lagrange-sinc basis set has been known to be complete.[67–69]

In the case of KLI, all the three orbitals form bound states. Therefore, they must be less sensitive to the basis set size compared to the HF and PBE cases, which apparently helps to enhance computational efficiency for MC methods demanding many virtual orbitals. In fact, we checked convergence of KLI orbitals with different scaling factors of the Lagrange-sinc basis set. For example, the orbital energy change was less than 0.0013 hartree as the scaling factor h decreases from 0.25 to 0.20 bohr, *i.e.*, the basis set size increases almost twice.

Asymptotic Behavior of the KLI Potential. Figure 2 compares the PZ-LDA exchange-correlation potential and the KLI exchange potential for a H_2 molecule. The LDA potential decays exponentially at a remote region, while the KLI potential follows a correct $-1/r$ behavior. We note that the nuclei

Table 1. Selected virtual orbitals of N_2. Scaling factor h of the Lagrange-sinc basis set is given in bohr.

	$1\pi_g$	$4\sigma_g$	$3\sigma_u$
HF aug-cc-pVQZ	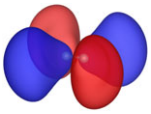	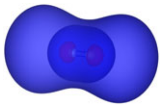	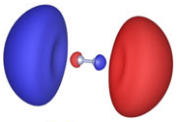
HF cc-pVDZ			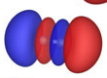
PBE aug-cc-pVQZ		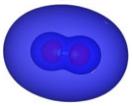	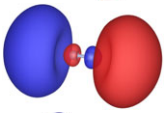
PBE cc-pVDZ			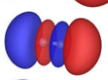
PBE Lagrange-sinc ($h = 0.25$)		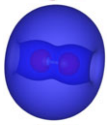	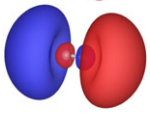
KLI Lagrange-sinc ($h = 0.25$)		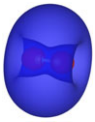	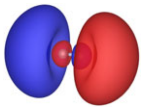
KLI Lagrange-sinc ($h = 0.20$)		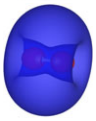	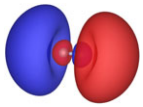

attractive potential is completely screened by the Hartree repulsive potential at a remote region, so that only the exchange-correlation potential remains there. As a result, LDA forms a shallow potential, leading to unbound virtual orbitals, whereas KLI provides an attractive potential to form the correct Rydberg states.

Figure 3(a) shows the occupied and virtual orbitals of H_2 computed from the KLI potential. Note that all the virtual orbitals are bound states with negative eigenvalues. Interestingly, the KLI orbitals look like the hydrogen atomic orbitals, though their degeneracies no longer remain. This shows that the KLI exchange potential removes the SIE and hence an electron at the remote region sees a single positive charge of nuclei screened only by the other electron, resulting in atomic-orbital-like Rydberg states. In contrast, HF gives only a single bound state that is the occupied orbital, as shown in Figure 3(b). Though the HF results also have hydrogen-like orbital shapes, there are also peculiar orbitals such as the left one with 0.047 hartree and the one with 0.327 hartree. This can be understood from the fact that unbound orbitals try to incorporate plane-wave-like nature within the given basis set. We expect that if a larger basis set is used, more peculiar orbitals will appear.

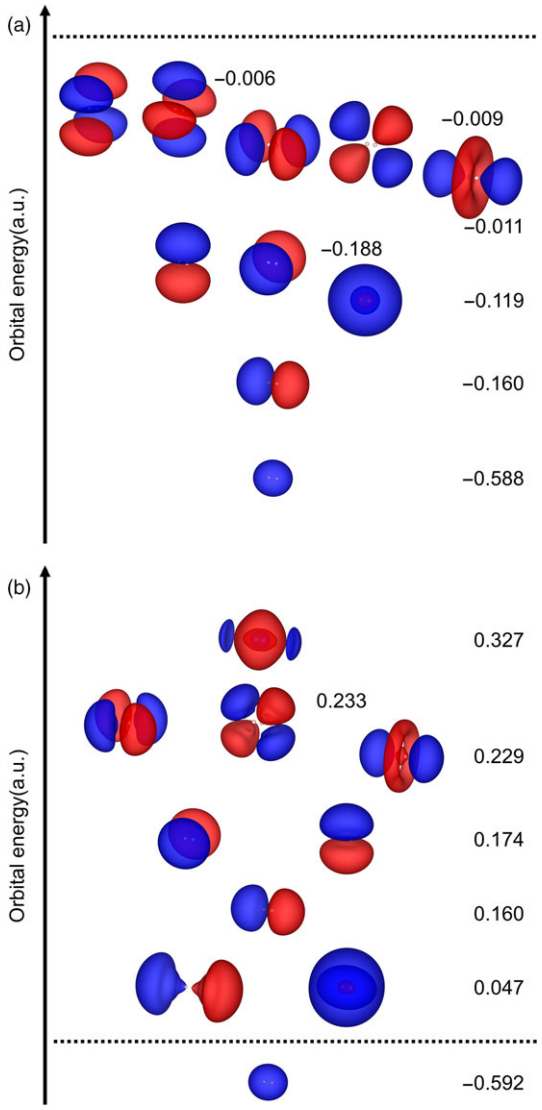

Figure 3. Occupied and virtual orbitals of H_2. (a) KLI results (h = 0.25 bohr). (b) HF results (aug-cc-pVQZ). The numbers indicate the eigenvalues of corresponding orbitals in hartree. The dotted line denotes the zero energy level.

Excitation Energy. The energy gaps between occupied and virtual orbitals are often regarded as the zeroth-order approximation of optical excitation energies for further excited state calculations. In particular, the transition energy from the HOMO to the lowest unoccupied molecular orbital (LUMO) is often used to estimate the lowest excitation of a given molecule. Table 2 compares the HOMO–LUMO energy gaps of small molecules computed from various methods and their corresponding experimental values. We used aug-cc-pVQZ for HF calculations, while the Lagrange-sinc basis set with the scaling of 0.25 bohr were used for DFT calculations. We note that the HF energy gaps are much larger than those from both KS results and experiments, which is because, by virtue of Koopmans' theorem, the HF energy gaps correspond to the fundamental gaps rather than optical excitation energies.

Unlike HF, however, a KS energy gap can be considered as the optical excitation energy. As discussed in the previous sections, LDA and GGA functionals produce upshifted orbital energies with respect to KLI results and thus they are likely to produce unbound virtual orbitals. An upshifted LUMO may be unnaturally diffuse so that it has a smaller SIE than the corresponding HOMO, leading to a small HOMO–LUMO energy gap. In particular, if it forms a unbound state, its energy is highly sensitive to the size of the basis set and thus the energy gap is meaningless. The results in Table 2 clearly show such a tendency. KLI gives larger energy gaps for all the molecules than LDA and PBE do, and its results are closer to the experimental values.[87] In the case of H_2, its LUMO from PZ-LDA/PBE is unbound and its HOMO–LUMO energy gap is much smaller than the KLI and experimental values.

We also investigated the effect of combining KLI exchange and PZ-LDA or PBE correlation energies on the energy gaps. Both cases yield similar results with the KLI exchange-only case. For CH_4, the results of the combined methods appear better than that of KLI. However, it does not mean that the PZ-LDA or PBE correlation functionals are good counterparts of the KLI exchange because no error cancelation between them is expected.

In this way, KLI enables us to obtain good approximated excitation energies as compared to the HF or conventional DFT methods. To further improve the KLI results, one may need to devise a correlation functional at the same level or to use them for post-HF-like calculations. For the latter case, Brillouin's theorem may be used for KLI orbitals. As the KLI exchange potential has been derived to effectively incorporate the HF exchange energy, we examine to what extent KLI orbitals satisfy Brillouin's theorem. To this end, we compare the KS total energy and the ground state energy from CIS

Table 2. The HOMO–LUMO energy gaps of small molecules (a.u.).[a]

	HOMO–LUMO energy gap						
	HF	PZ-LDA	PBE	KLIx	KLIx PZc	KLIx PBEc	Vertical excitation energy[82]
H_2	0.639	0.392	0.395	0.429	0.449	0.446	0.42($^3\Sigma_u^+$) / 0.46($^1\Pi_u$)
CO	0.616	0.250	0.257	0.264	0.267	0.259	0.23($^3\Pi$) / 0.31($^1\Pi$)
N_2	0.684	0.300	0.304	0.318	0.318	0.314	0.28($^3\Sigma_u^+$) / 0.34($^1\Pi_g$)
CH_4	0.571	0.347	0.345	0.382	0.408	0.407	0.40($^3T_2$) / 0.41($^1T_2$)

[a] aug-cc-pVQZ basis set was used for HF calculations, and the Lagrange-sinc basis set with the scaling of 0.25 bohr was used for DFT calculations.

Table 3. Comparison of KS total energy (E_{KS}), $\langle\Psi_0|\hat{H}|\Psi_0\rangle$ (E_0), and CIS ground state energy (E_{CIS}) (a.u.)

	KLI			PBE		
	E_{KS}	E_0	E_{CIS}	E_{KS}	E_0	E_{CIS}
H_2	−1.124	−1.124	−1.124	−1.156	−1.123	−1.123
CO	−21.268	−21.268	−21.269	−21.679	−20.574	−20.578
N_2	−19.476	−19.476	−19.476	−19.904	−19.468	−19.468
CH_4	−7.852	−7.852	−7.853	−8.083	−7.848	−7.849

calculations, as shown in Table 3. The results were produced by our code with the scaling factor of 0.25 bohr. In CIS calculations, we include 15 orbitals, which are all valence orbitals, and several lowest virtual orbitals. For comparison, we used both PBE and KLI orbitals.

In the case of KLI, E_{KS} is exactly the same as E_0, because the total KS energy of KLI must be identical to the HF energy computed from KLI orbitals as follows:

$$\begin{aligned} E_{KS}^{KLI}[\{\varphi_i\}] &= \sum_i \langle i|\hat{T}|i\rangle + \int d\mathbf{r} v_{ext}(\mathbf{r})\rho(\mathbf{r}) \\ &+ \frac{1}{2}\int\int d\mathbf{r}d\mathbf{r}' \frac{\rho(\mathbf{r})\rho(\mathbf{r}')}{|\mathbf{r}-\mathbf{r}'|} + E_x^{KLI}[\{\varphi_i\}] \\ &= E_0^{HF}[\{\varphi_i\}], \end{aligned} \tag{31}$$

where the last equality comes from that $E_x^{KLI} = E_x^{HF}$. Therefore, the CIS correction of KLI to the ground state is negligible within 10^{-3} hartree, as can be seen from Table 3. In contrast, E_{KS} of PBE is significantly different from E_0, because KS orbitals are not the eigenfunctions of the corresponding Fock operator. However, E_0 of PBE is also very close to E_{CIS}. This result shows that Brillouin's theorem is valid for CIS calculations using KLI orbitals on the order of 10^{-3} hartree.

Conclusion

We implemented the KLI version of EXX potential in our DFT code, which allowed us to obtain the self-interaction free molecular orbitals. We performed DFT and HF calculations for small molecules and compared the energies and shapes of the resulting orbitals with each other. For occupied orbitals, KLI gives similar energies and shapes with those of HF. In particular, the KLI exchange potential has the correct $-1/r$ asymptotic behavior and thus its HOMO energy obeys Koopman's theorem like HF. For virtual orbitals, however, KLI orbitals have a physically different meaning from the HF orbitals. The former gives an approximated optical excitation energy, while the latter gives an approximated electron affinity. Therefore, KLI virtual orbitals are likely to form bound states with negative eigenvalues and so relatively less sensitive to the size of basis set, whereas HF virtual orbitals tend to be diffuse as much as the basis set allows.

LDA and GGA functionals have shallow and upshifted exchange-correlation potential with exponentially decaying asymptotic behavior. As a result, their orbital energies with small eigenvalues are almost upshifted with respect to the KLI results, but those with high eigenvalues form unbound states like HF. The KLI HOMO–LUMO energy gaps show better excitation energies than the other methods. Combining the KLI exchange with the LDA or GGA correlation functionals results in similar energy gaps with the KLI-only case. We expect that orbital-dependent correlation functionals (*e.g.*, the OEP potential for correlation energy[32–37]) may improve the results.

We note that the ground state energy from CIS calculations using KLI orbitals is equal to the KS total energy of KLI within 10^{-3} hartree. Therefore, Brillouin's theorem is approximately valid to a Slater determinant made of KLI orbitals. Consequently, KLI orbitals provide accurate zeroth-order approximation for electronic excitation energies and thus their Slater determinant forms a good reference to construct many-electron wavefunctions through the configuration interaction expansion. At present, we are developing MC methods in the basis of KLI orbitals as a new promising approach for high-level quantum calculations.

Acknowledgments. This work was supported by Basic Science Research Programs (NRF-2012R1A1A1004154), the EDISON Program (NRF-2012M3C1A6035359), and the

MIR center (No. 20090083525) through the NRF funded by the Korea Government (MSIP). The authors would like to acknowledge the support from the KISTI supercomputing center for computing time (KSC-2013-C1-028). WYK is also grateful for financial support from the Chung-Am Fellowship and the EWon Assistant Professorship.

References

1. K. Burke, *J. Chem. Phys.* **2012**, *136*, 150901.
2. A. D. Becke, *J. Chem. Phys.* **2014**, *140*, 18A301.
3. E. Engel, R. M. Dreizler, *Density Functional Theory—An Advanced Course, Theoretical and Mathematical Physics*, Springer, Berlin; Heidelberg, 2011.
4. V. Polo, E. Kraka, D. Cremer, *Mol. Phys.* **2002**, *100*, 1771.
5. T. Tsuneda, K. Hirao, *J. Chem. Phys.* **2014**, *140*, 18A513.
6. E. J. Baerends, O. V. Gritsenko, R. van Meer, *Phys. Chem. Chem. Phys.* **2013**, *15*, 16408.
7. R. Sharp, G. Horton, *Phys. Rev.* **1953**, *90*, 317.
8. J. Talman, W. Shadwick, *Phys. Rev. A* **1976**, *14*, 36.
9. M. Norman, D. Koelling, *Phys. Rev. B* **1984**, *30*, 5530.
10. S. Kümmel, J. Perdew, *Phys. Rev. B* **2003**, *68*, 035103.
11. S. Kümmel, L. Kronik, *Rev. Mod. Phys.* **2008**, *80*, 3.
12. J. B. Krieger, Y. Li, G. J. Iafrate, *Phys. Lett. A* **1990**, *148*, 470.
13. J. Krieger, Y. Li, G. Iafrate, *Phys. Rev. A* **1992**, *45*, 101.
14. J. Krieger, Y. Li, G. Iafrate, *Phys. Rev. A* **1992**, *46*, 5453.
15. J. B. Krieger, Y. Li, G. J. Iafrate, In *Density Functional Theory*. NATO ASI Series, Vol. *337*, E. K. U. Gross, R. M. Dreizler Eds., Springer, Boston, MA, 1995, p. 191.
16. F. Della Sala, A. Görling, *J. Chem. Phys.* **2001**, *115*, 5718.
17. F. Della Sala, A. Görling, *J. Chem. Phys.* **2002**, *116*, 5374.
18. F. Della Sala, A. Görling, *J. Chem. Phys.* **2003**, *118*, 10439.
19. O. Gritsenko, E. Baerends, *Phys. Rev. A* **2001**, *64*, 042506.
20. M. Grüning, O. V. Gritsenko, E. J. Baerends, *J. Chem. Phys.* **2002**, *116*, 6435.
21. I. G. Ryabinkin, A. A. Kananenka, V. N. Staroverov, *Phys. Rev. Lett.* **2013**, *111*, 013001.
22. S. V. Kohut, I. G. Ryabinkin, V. N. Staroverov, *J. Chem. Phys.* **2014**, *140*, 18A535.
23. J. P. Perdew, *AIP Conf. Proc.* **2001**, *577*, 1.
24. J. Tao, J. Perdew, V. Staroverov, G. Scuseria, *Phys. Rev. Lett.* **2003**, *91*, 146401.
25. M. Hellgren, U. von Barth, *Phys. Rev. B* **2007**, *76*, 075107.
26. A. Heßelmann, A. Görling, *Mol. Phys.* **2010**, *108*, 359.
27. A. Heßelmann, A. Görling, *Mol. Phys.* **2011**, *109*, 2473.
28. A. Heßelmann, A. Görling, *Phys. Rev. Lett.* **2011**, *106*, 093001.
29. M. Hellgren, D. R. Rohr, E. K. U. Gross, *J. Chem. Phys.* **2012**, *136*, 034106.
30. P. Verma, R. J. Bartlett, *J. Chem. Phys.* **2012**, *136*, 044105.
31. P. Bleiziffer, A. Heßelmann, A. Görling, *J. Chem. Phys.* **2013**, *139*, 084113.
32. P. Mori-Sánchez, Q. Wu, W. Yang, *J. Chem. Phys.* **2005**, *123*, 62204.
33. I. V. Schweigert, V. F. Lotrich, R. J. Bartlett, *J. Chem. Phys.* **2006**, *125*, 104108.
34. I. Grabowski, V. Lotrich, R. J. Bartlett, *J. Chem. Phys.* **2007**, *127*, 154111.
35. S. Grimme, L. Goerigk, R. F. Fink, *Wiley Interdiscip. Rev. Comput. Mol. Sci.* **2012**, *2*, 886.
36. I. Grabowski, E. Fabiano, F. Della Sala, *Phys. Rev. B* **2013**, *87*, 075103.
37. I. Grabowski, E. Fabiano, A. M. Teale, S. Śmiga, A. Buksztel, F. Della Sala, *J. Chem. Phys.* **2014**, *141*, 024113.
38. B. B. Miehlich, H. Stoll, A. Savin, *Mol. Phys.* **1997**, *91*, 527.
39. T. Leininger, H. Stoll, H.-J. Werner, A. Savin, *Chem. Phys. Lett.* **1997**, *275*, 151.
40. J. Gräfenstein, D. Cremer, *Phys. Chem. Chem. Phys.* **2000**, *2*, 2091.
41. J. Gräfenstein, D. Cremer, *Chem. Phys. Lett.* **2000**, *316*, 569.
42. R. Takeda, S. Yamanaka, K. Yamaguchi, *Chem. Phys. Lett.* **2002**, *366*, 321.
43. R. Pollet, A. Savin, T. Leininger, H. Stoll, *J. Chem. Phys.* **2002**, *116*, 1250.
44. R. Takeda, S. Yamanaka, K. Yamaguchi, *Int. J. Quantum Chem.* **2004**, *96*, 463.
45. S. Gusarov, P.-Å. Malmqvist, R. Lindh, B. O. Roos, *Theor. Chem. Acc.* **2004**, *112*, 84.
46. J. Toulouse, F. Colonna, A. Savin, *Phys. Rev. A* **2004**, *70*, 062505.
47. J. Gräfenstein, D. Cremer, *Mol. Phys.* **2005**, *103*, 279.
48. S. Yamanaka, K. Nakata, T. Ukai, T. Takada, K. Yamaguchi, *Int. J. Quantum Chem.* **2006**, *106*, 3312.
49. S. Yamanaka, K. Nakata, T. Takada, K. Kusakabe, J. M. Ugalde, K. Yamaguchi, *Chem. Lett.* **2006**, *35*, 242.
50. S. Grimme, *Chem. Phys. Lett.* **1996**, *259*, 128.
51. S. Grimme, M. Waletzke, *J. Chem. Phys.* **1999**, *111*, 5645.
52. P. Bouř, *Chem. Phys. Lett.* **2001**, *345*, 331.
53. L. Veseth, *J. Chem. Phys.* **2001**, *114*, 8789.
54. T. Hupp, B. Engels, F. Della Sala, A. Görling, *Chem. Phys. Lett.* **2002**, *360*, 175.
55. T. Hupp, B. Engels, F. Della Sala, A. Görling, *Z. Phys. Chem.* **2003**, *217*, 133.
56. T. Hupp, B. Engels, A. Görling, *J. Chem. Phys.* **2003**, *119*, 11591.
57. C. Gutle, A. Savin, J. B. Krieger, J. Chen, *Int. J. Quantum Chem.* **1999**, *75*, 885.
58. C. Gutlé, J. Heully, J. Krieger, A. Savin, *Phys. Rev. A* **2002**, *66*, 012504.
59. S. Choi, K. Hong, J. Kim, W. Y. Kim, *J. Chem. Phys.* **2015**, in press.
60. W. Kohn, L. J. Sham, *Phys. Rev.* **1965**, *140*, A1133.
61. S. Kümmel, J. Perdew, *Phys. Rev. Lett.* **2003**, *90*, 043004.
62. J. Garza, J. A. Nichols, D. A. Dixon, *J. Chem. Phys.* **2000**, *112*, 7880.
63. E. Engel, A. Höck, R. Dreizler, *Phys. Rev. A* **2000**, *62*, 042502.
64. S. Hirata, S. Ivanov, I. Grabowski, R. J. Bartlett, K. Burke, J. D. Talman, *J. Chem. Phys.* **2001**, *115*, 1635.
65. G. J. Iafrate, J. B. Krieger, *J. Chem. Phys.* **2013**, *138*, 094104.
66. J. Slater, *Phys. Rev.* **1951**, *81*, 385.
67. D. Baye, *Phys. Status Solidi* **2006**, *243*, 1095.
68. K. Varga, S. T. Pantelides, *Phys. Status Solidi* **2006**, *243*, 1110.
69. K. Varga, Z. Zhang, S. Pantelides, *Phys. Rev. Lett.* **2004**, *93*, 1.
70. D. Sundholm, *J. Chem. Phys.* **2005**, *122*, 194107.
71. J. Jusélius, D. Sundholm, *J. Chem. Phys.* **2007**, *126*, 094101.
72. F. Bloch, *Z. Phys.* **1929**, *57*, 545.
73. P. A. M. Dirac, *Proc. Cambridge Phil. Soc.* **1930**, *26*, 376.
74. J. P. Perdew, A. Zunger, *Phys. Rev. B* **1981**, *23*, 5048.
75. J. P. Perdew, K. Burke, M. Ernzerhof, *Phys. Rev. Lett.* **1996**, *77*, 3865.

76. R. D. Johnson, III. NIST Computational Chemistry Comparison and Benchmark Database, NIST Standard Reference Database Number 101, Release 16a. URL http://cccbdb.nist.gov/ (accessed December 12, 2014).
77. M. J. Frisch, G. W. Trucks, H. B. Schlegel, G. E. Scuseria, M. A. Robb, J. R. Cheeseman, G. Scalmani, V. Barone, B. Mennucci, G. A. Petersson, H. Nakatsuji, M. Caricato, X. Li, H. P. Hratchian, A. F. Izmaylov, J. Bloino, G. Zheng, J. L. Sonnenberg, M. Hada, M. Ehara, K. Toyota, R. Fukuda, J. Hasegawa, M. Ishida, T. Nakajima, Y. Honda, O. Kitao, H. Nakai, T. Vreven, J. A. J. Montgomery, J. E. Peralta, F. Ogliaro, M. Bearpark, J. J. Heyd, E. Brothers, K. N. Kudin, V. N. Staroverov, R. Kobayashi, J. Normand, K. Raghavachari, A. Rendell, J. C. Burant, S. S. Iyengar, J. Tomasi, M. Cossi, N. Rega, M. J. Millam, M. Klene, J. E. Knox, J. B. Cross, V. Bakken, C. Adamo, J. Jaramillo, R. Gomperts, R. E. Stratmann, O. Yazyev, A. J. Austin, R. Cammi, C. Pomelli, J. W. Ochterski, R. L. Martin, K. Morokuma, V. G. Zakrzewski, G. A. Voth, P. Salvador, J. J. Dannenberg, S. Dapprich, A. D. Daniels, Ö. Farkas, J. B. Foresman, J. V. Ortiz, J. Cioslowski, D. J. Fox, *Gaussian 09, Revision A.02*, Gaussian, Inc., Wallingford, CT, 2009.
78. D. Corso. THEOS. URL http://theossrv1.epfl.ch/Main/Pseudopotentials (accessed December 12, 2014).
79. K. Momma, F. Izumi, *J. Appl. Crystallogr.* **2011**, *44*, 1272.
80. P. E. Cade, *J. Chem. Phys.* **1966**, *44*, 1973.
81. A. Szabo, N. S. Ostlund, *Modern Quantum Chemistry: Introduction to Advanced Electronic Structure Theory*, McGraw-Hill, New York, 1989, p. 192.
82. Y. Kim, M. Stadele, R. M. Martin, *Phys. Rev. A* **1999**, *60*, 3633.
83. R. Van Meer, O. V. Gritsenko, E. J. Baerends, *J. Chem. Theory Comput.* **2014**, *10*, 4432.
84. F. Della Sala, A. Görling, *Phys. Rev. Lett.* **2002**, *89*, 033003.
85. M. Weimer, F. Della Sala, A. Görling, *Chem. Phys. Lett.* **2003**, *372*, 538.
86. O. V. Gritsenko, E. J. Baerends, *J. Chem. Phys.* **2004**, *120*, 8364.
87. Note that the HOMO–LUMO energy gap may correspond to a value between the lowest singlet and triplet excitation energies, because the energy gap does not assume any spin-dependent excitation.
88. T. Grabo, M. Petersilka, E. K. U. Gross, *J. Mol. Struct. (Theochem)* **2000**, *501–502*, 353.
89. R. G. Parr, W. Yang, *Density-Functional Theory of Atoms and Molecules*, Oxford University Press, New York, 1989.